



Article

Performance Evaluation of Two Commercially Available Portable Spectrometers to Non-Invasively Determine Table Grape and Peach Quality Attributes

Irwin R. Donis-González ^{1,*}, Constantino Valero ^{2,†} , Md Abdul Momin ^{1,†}, Amanjot Kaur ³ and David C. Slaughter ¹

¹ Biological and Agricultural Engineering Department, University of California-Davis, Davis, CA 95616, USA; mamomin@ucdavis.edu (M.A.M.); dcslaughter@ucdavis.edu (D.C.S.)

² Departamento Ingeniería Agroforestal, Universidad Politécnica de Madrid, 28040 Madrid, Spain; constantino.valero@upm.es

³ Department of Plant Sciences, University of California-Davis, Davis, CA 95616, USA; akskaur@ucdavis.edu

* Correspondence: irdonisgon@ucdavis.edu; Tel.: +1-530-752-898-6

† These authors contributed equally to this manuscript.

Received: 3 December 2019; Accepted: 16 January 2020; Published: 19 January 2020



Abstract: Near-infrared (NIR) spectroscopy has been used to non-destructively and rapidly evaluate the quality of fresh agricultural produce. In this study, two commercially available portable spectrometers (F-750: Felix Instruments, WA, USA; and SCiO: Consumer Physics, Tel Aviv, Israel) were evaluated in the wavelength range between 740 and 1070 nm to non-invasively predict quality attributes, including the dry matter (DM), and total soluble solids (TSS) content of three fresh table grape cultivars ('Autumn Royal', 'Timpson', and 'Sweet Scarlet') and one peach cultivar ('Cassie'). Prediction models were developed using partial least-square regression (PLSR) to correlate the NIR absorbance spectra with the invasive quality measurements. In regard to grapes, the best DM prediction models yielded an R^2 of 0.83 and 0.81, a ratio of standard error of performance to standard deviation (RPD) of 2.35 and 2.29, and a root mean square error of prediction (RMSEP) of 1.40 and 1.44; and the best TSS prediction models generated an R^2 of 0.97 and 0.95, an RPD of 5.95 and 4.48, and an RMSEP of 0.53 and 0.70 for the F-750 and SCiO spectrometers, respectively. Overall, PLSR prediction models using both spectrometers were promising to predict table grape quality attributes. Regarding peach, the PLSR prediction models did not perform as well as in grapes, as DM prediction models resulted in an R^2 of 0.81 and 0.67, an RPD of 2.24 and 1.74, and an RMSEP of 1.28 and 1.66; and TSS resulted in an R^2 of 0.62 and 0.55, an RPD of 1.55 and 1.48, and an RMSEP of 1.19 and 1.25 for the F-750 and SCiO spectrometers, respectively. Overall, the F-750 spectrometer prediction models performed better than those generated by using the SCiO spectrometer data.

Keywords: grape; peach; dry matter; total soluble solids; NIR spectroscopy; partial least-square regression

1. Introduction

Fruits and vegetables produced in California have a paramount impact on the national economy [1]. Among the top twenty agricultural commodities produced in this state, grapes (*Vitis vinifera* L.) are the number one fresh fruit with a total market value of more than 5.8 billion dollars (2017). California also leads the nation's production of many other commodities—meaning that it generates 99 percent or more—among which, peaches (*Prunus persica* L.) and grapes are again included [1]. Consequently, fruit producers and farm technicians are interested in devices capable of non-destructively measuring the internal quality of these fruits [2], and frequently ask for scientific evidence to local extension services.

With the objective of supplying a high and consistent quality of fresh fruits and vegetables, various non-destructive technologies including optical (e.g., computer vision system, and spectroscopy) and electromagnetic techniques (e.g., magnetic resonance imaging) have been evaluated [2]. Among these technologies, visible (VIS) and near-infrared (NIR) spectroscopy is a rapid, non-destructive and simple method that has gained attraction, as it has been widely used to infer internal and external physiochemical constituents, and quality attributes of fresh agricultural produce [3,4]. Spectroscopic techniques usually study the VIS (380–720 nm) and NIR (780–2500 nm) wavelengths of the electromagnetic spectrum based on absorption of energy from molecules or chemical constituents of the produce within these regions. Signals of major structures and functional groups of organic compounds, such as the O-H, C-H, and N-H structures, are detected within the NIR range [5]. When incident light contacts the surface of a fruit, the light undergoes spectral changes as it interacts with the fruit at a molecular level (at a depth of 1–2 cm below the peel) per a sample's chemical composition and internal organic matter. Molecules are excited and experience shifts in their energy levels or states. Consequently, the light is reflected, transmitted, or absorbed [6]. A specific molecule, such as the water molecule, can partially or fully absorb the light at a given wavelength or wavelength range resulting in the absorption spectrum.

The resulting VIS/NIR, VIS, or NIR spectra of a fresh fruit or vegetable are frequently convoluted due to several interfering factors: Water highly absorbs NIR radiation; low signal-to-noise ratio (SNR) (i.e., measure of the quality or resolution of a peak); high overlap of combination (i.e., simultaneous stretching and excitation bands) and overtones (i.e., bands due to transitions of molecules from ground to higher energy levels) bands; scattering of light (e.g., specular or mirror-like reflectance); instrumental noise; and complex constitution of the biological sample such as a fruit tissue heterogeneities [5,7–10]. Chemometrics, or computational chemistry, and mathematical and multivariate statistical tools (e.g., partial least-squares regression) and spectral pre-processing treatments are essential to extract the fruit quality relevant information from the convoluted VIS/NIR spectrum [8,11–13]. VIS/NIR spectral data combined with chemometric analysis techniques have been applied to assess maturity, appearance, and sweetness of several agricultural produce, therefore ensuring that the produce meets specific quality standards [5,9,14].

Harvest timing of table grapes and peaches is an important attribute, which has proven to be challenging to predict and/or estimate. Typically, fruit growers subjectively and visually estimate harvesting time by observing color changes on the fruit. In some cases, color changes are slight, undetectable and/or do not reflect the overall maturity of the crop. In addition, growers typically apply laborious postharvest processing, and/or biochemical assays with expensive chemicals and specialized lab equipment. Premature and/or delayed harvesting can negatively impact yield and quality, and may lead to quantitative, qualitative, and nutritional postharvest losses. Several studies have been performed with promising results to objectively assess table grape and peach maturity and quality attributes, using NIR spectroscopic techniques. Research performed by [15–17] stated that NIR spectroscopy techniques have the ability to rapidly and accurately predict several vineyard table grape quality attributes, including their total soluble solids (TSS) content, and can potentially be used to infer and monitor table grape maturity/ripeness in the field. In addition, portable VIS/NIR systems to non-destructively and rapidly predict fresh berry and homogenized sample quality parameters has also been developed and tested by [18], resulting in classification models with a high accuracy rate of 89% for TSS and 83% for acidity. To evaluate the maturity and quality of peaches, various physical and chemical properties such as firmness, TSS, dry matter (DM) and titratable acidity were successfully investigated using NIR spectroscopy methods, as seen in [19–22].

The applications of portable NIR produce quality spectrometers have not been fully addressed, especially under practical real-life conditions. To date, most studies have focused in laboratory based spectrometers to non-destructively predict various quality attributes [15] while only in some studies comparisons with portable devices have been performed [23,24]. Recent advancements in sensorics and microelectronics have resulted in the creation of hand-held, commercially available NIR produce

quality spectrometers of several brands, such as the F-750 (Felix Instruments, Camas, WA, USA), and SCiO (Consumer Physics, Tel Aviv, Israel). The latter belongs to the recent category of miniaturized spectrometers, with increasing interest nowadays due to their potential application inside mobile phones [25,26]; its capabilities have been applied to a wide range of studies, from cultivar detection on seeds [27] to the characterization of pharmacy tablets [23]. Therefore, potential users in particular agri-food producers, technicians, and extension personnel are interested in scientific studies and information regarding the prediction performance, and practical application of these equipment. These tools should be accurate, robust, and easy to use to allow real-time and in-field measurement conditions. For in-field non-destructive fruit quality attribute prediction, spectrometers should tolerate differences in fruit maturity, color, varieties, and environment. Thus, the goal of this study was to evaluate the potential of two commercially available hand-held portable non-invasive VIS/NIR produce quality spectrometers, including the Felix-750 and SCiO, to predict quality attributes (DM and TSS) in fresh table grapes and peach fruits.

2. Materials and Methods

2.1. Fruit Samples

Table grapes and peach fruits were selected among other species for this experiment due to two main reasons: First, their economic importance in local and national economy, and, second, their different size, which may affect light diffusion in their internal tissues and, therefore, final quality estimation. Samples were hand harvested from commercial grower fields on July 2017 in Bakersfield, in the case of table grapes, and in Esparto, CA, USA, in the case of peaches. Table grape samples included a total of 450 single berries from three cultivars containing different skin colors, 'Autumn Royal' (purple), 'Timpson Seedless' (green), and 'Sweet Scarlett' (red) (150 berries per cultivar); and 150 peach fruits from one cultivar ('Cassie'), as summarized in Table 1. Immediately after harvest, samples were transported in a cooler to the Postharvest Engineering laboratory at UC Davis and stored in a walk-in cold room (0 °C) before spectral measurements.

Table 1. Descriptive statistics for table grape and peach sample quality attributes.

| Parameters | DM (%) | | | | TSS (°Brix) | | | |
|----------------|-------------|-------|-------|-------|-------------|-------|-------|-------|
| | Table Grape | | | Peach | Table Grape | | | Peach |
| | Purple | Green | Red | | Purple | Green | Red | |
| No. of samples | 150 | 150 | 150 | 150 | 150 | 150 | 150 | 150 |
| Minimum | 9.09 | 6.12 | 7.70 | 9.01 | 8.2 | 4.35 | 6.00 | 7.30 |
| Maximum | 23.85 | 24.61 | 22.46 | 30.72 | 17.55 | 21.1 | 20.6 | 17.85 |
| Mean | 14.45 | 15.89 | 17.32 | 17.04 | 12.4 | 14.48 | 16.15 | 12.57 |
| Std. deviation | 2.74 | 3.88 | 2.64 | 3.11 | 2.15 | 3.61 | 2.49 | 1.93 |

DM = dry matter, TSS = total soluble solids.

2.2. Fresh Fruit Spectral Measurements

Two commercially available hand-held produce quality spectrometers, as described in Table 2, were used in this study. The SCiO spectrometer was a brand new piece of equipment, acquired for the purpose of this experiment, while the F-750 spectrometer have been used before for other scientific projects at the Biological and Agricultural Engineering Dept. of University of California-Davis, having all the setup and calibration procedures adequately updated. In order to create temperature-compensated calibration models, reflectance spectra using the F-750 spectrometer were acquired twice on opposite sides on the surface of each sample (each berry in the case of grapes, and each peach fruit), at three different temperatures (0, 10, and 20 °C). Fruit samples were allowed to equilibrate in different cold rooms at the desired temperature for a minimum of 2 h, and spectra acquisition was performed inside each cold room. The same process was repeated using the SCiO spectrometer but, due to its short

battery life, this was only performed at two different temperatures (0 and 20 °C). For each sample, a mean spectrum was calculated by averaging the total scan spectra (6 for the F-750 spectrometer, and 4 for the SCiO spectrometer) collected for each berry or fruit at the different temperatures.

In the case of the F-750 spectrometer, recorded spectral data for all of the fruit samples were transferred to a laptop computer (Intel Core i7-7700HQ CPU 2.80 GHz 16.0 GB RAM) using a Secure Digital (SD) card and the 'F-750 Model Builder' software Version 1.3.0.177 (Felix Instruments, Camas, WA, USA), and saved using a Comma-Separated Values (CSV) file format for later spectral processing. For the SCiO spectrometer, measured reflectance spectra were stored in the manufactures cloud service (Consumer Physics; Tel Aviv, Israel), using an iPhone 6s (Apple Inc. Cupertino, CA, USA), and saved in a laptop computer using a CSV file format for later spectral processing. Ultimately, reflectance spectra from the SCiO spectrometer were transformed to absorbance spectra, using Equation (1).

$$\text{Absorbance} = \log (1/\text{Reflectance}) \quad (1)$$

After spectral measurement and transformation were performed, data were imported into Matlab R2018a (version 9.4 Release March 2018, The Mathworks, Natick, Boston, MA, USA). Spectra data wavelength range selection, pre-processing, data analysis and visualization, and partial least-square (PLSR) regression calibration and prediction model development were performed in the Matlab environment and the PLSR Toolbox (version 7, Eigenvector Research, Inc. 2012, Manson, WA, USA).

Table 2. Technical specifications of produce quality spectrometers used in the study.

| Characteristics | Device Model (Manufacturer) | |
|---|--|---|
| | F-750 (Felix Instruments, Natick, WA, USA) | SCiO (Consumer Physics, Tel Aviv, Israel) |
| Full range (nm) | 285–1200 | 740–1070 |
| Usable range (nm) in this study | 741–1071 | 740–1070 |
| Resolution (nm) | 3 | 1 |
| Display | LCD screen | Phone |
| Interface | PC based via USB and SD card | iPhone 5 and above with iOS 9 or higher; Android 4.3 or higher |
| Measurement | Reflectance, absorbance, first derivative | Reflectance |
| Power | Four 3100 mAh lithium-ion battery (easy to replace rechargeable batteries) | Rechargeable internal lithium polymer battery |
| Battery life (Approximate number of measurements) | 1600 | <500 |
| Dimensions (mm) | 180.34 × 120.65 × 44.45 | 67.7 × 40.2 × 18.8 |
| Weight (g) | 1050 | 35 |
| Price (US\$) | 8500 (Equipment and local training software) | 500 (Equipment) 2950 (Online scientific package) |

2.3. Spectral Data Wavelength Range Selection, and Pre-Processing

Acquired spectra from a biological sample, such as a fresh fruit, typically contain high- and/or low-frequency interferences and irrelevant information, which might influence prediction performance, and accurate development of calibration/prediction models. Non-relevant information can be present due to intrinsic equipment electronic noise, dark current, shot and readout noise, sample background variations, unwanted incidence light (stray light) and scattering, changes in light intensity, and non-uniform distribution of light over the scanned surface. Defining the usable wavelength range for each spectrometer, and spectral pre-processing of the originally acquired spectra is imperative to remove any irrelevant information within the spectra, and to develop reliable and stable calibration and predictions models [3,28,29]. Therefore, due to differences in color between samples, the VIS range of the F-750 spectrometer was not included in the development of quality attribute prediction models. In addition, the usable wavelength range for both spectrometers (740–1070 nm) was further defined by evaluating their performance (SNR, and signal variation with room temperature) with 25.3 mm diameter Polytetrafluoroethylene (Teflon) spheres as reference standards/phantoms on a separate experiment. These spheres are chemically inert, moisture and high-heat resistant. Spectra of the reference sphere were measured on top of the Teflon sphere at three different room temperatures

(0, 10, and 20 °C). For each sphere, the spectrum was measured 5 times in sequence, and a total of 25 spectrums (3 repetitions of 5 measurements) were recorded per temperature. A total of 75 spectrums were analyzed per spectrophotometer in the spectral range 740–1070 nm. The average coefficient of variation (CV) of the measured spectrums wavelength by wavelength for each temperature was calculated, as well as the SNR.

Also, with the aim of improving the calibration models, several well-known mathematical pre-processing techniques were applied to the originally acquired spectra (original), including the Standard Normal Variate (SNV), Orthogonal Signal Correction (OSC), Multiplicative Scattering Correction (MSC), First Derivative (FD), and Second Derivative (SD), and smoothing using the Savitzky–Golay (SG) algorithm [7,13].

2.4. Fruit Quality Attribute Measurements (DM, and TSS)

After spectral measurements, each sample fruit was immediately processed to estimate its DM (%) and TSS (°Brix) content, as reference measurements (quality attributes). The initial weight of the approximate one-quarter of each fruit was recorded and then dehydrated until constant mass was reached in an oven at 110 °C temperature. The DM content of each sample was then calculated by dividing the dry weight by its corresponding initial (wet) weight.

The second half of each peach sample fruit was juiced using a juice extractor (Big Mouth Pro Juice Extractor, Hamilton Beach, Glen Allen, VA, USA) and thoroughly mixed. The second half of each table grape sample fruits were manually squeezed by firmly pressing each fruit, and thoroughly mixed. Then, to measure the TSS content, a juice aliquot containing 0.3 mL of juice was placed onto a digital hand-held refractometer (Atago PAL-1, Tokyo 105-0011, Japan) with an accuracy of $\pm 0.2\%$, as specified by the manufacturer. DM and TSS reference measurements were performed in duplicate, while fruits were held at a 20 °C constant temperature.

2.5. Modeling the Relationship between Spectral Data and Quality Attributes

Partial Least-squares Regression (PLSR) was employed to model the relationship between the spectral and invasive quality attribute data (DM, and TSS) of both fruits (table grapes, and peach). PLSR essentially predict each quality attribute vector (Y) from the spectral matrix (X) by modeling the shared structure between the two, and extracting a group of orthogonal (or statistically independent) latent variables (LV), while simultaneously decomposing X and Y [11]. This translates into finding components along directions of maximal covariance between X and Y . For the regression then the focus is concentrated on these orthogonal factors to model the relationship [7].

Data were categorized into spectra and quality attributes matrices per the PLSR algorithm and randomly divided into a 75% for the calibration set, and 25% for the prediction. Cross-Validation (CV) divided the calibration set into 10-folds with 20 iterations using the Venetian blinds method. When predicting quality attribute values for the prediction set, the PLSR algorithm calculates new LV estimates as linear combinations of the original variables from the spectra matrix and uses these estimates as predictors. Minimum value for the root-mean square error of cross-validation (RMSECV) is used to select the optimum number of latent variables (LV) (max was fixed as 20) used to internally calculate the best model for each quality attribute [30–32]. RMSECV is obtained by comparing the predicted trait value with its reference value. In addition to the number of LV, PLSR statistical parameters to estimate performance of the selected model included R^2_{cal} and R^2_{pred} (the coefficient of determination for calibration and prediction, respectively), SEC and SEP (standard error of calibration and prediction, respectively), RPD (residual predictive deviation), and Bias (average difference between predicted and actual values). PLSR models with maximum R^2 and RPD, and lowest SEC, SEP and Bias values were selected as the optimum pre-processing method and best regression calibration models [3,33–36].

3. Results and Discussion

Depicted in Figure 1 are the original spectra of the samples, averaged per cultivar (green, purple and red grapes, and peaches), acquired with the SCiO spectrometer. Even though this device records data in the NIR region between 740 and 1070 nm, larger differences were observed between species than between varieties, having peach spectra a broader light absorption range than the grape spectrum. This behavior was also corroborated by NIR+VIS spectra acquired with the Felix device (not shown), where differences also in the VIS region were larger between fruit species due to their respective skin and flesh colors. Consequently, data analyses were done from this point on combining the spectra of all table grapes, with the aim of obtaining robust global models for each fruit species, and not only for single cultivars.

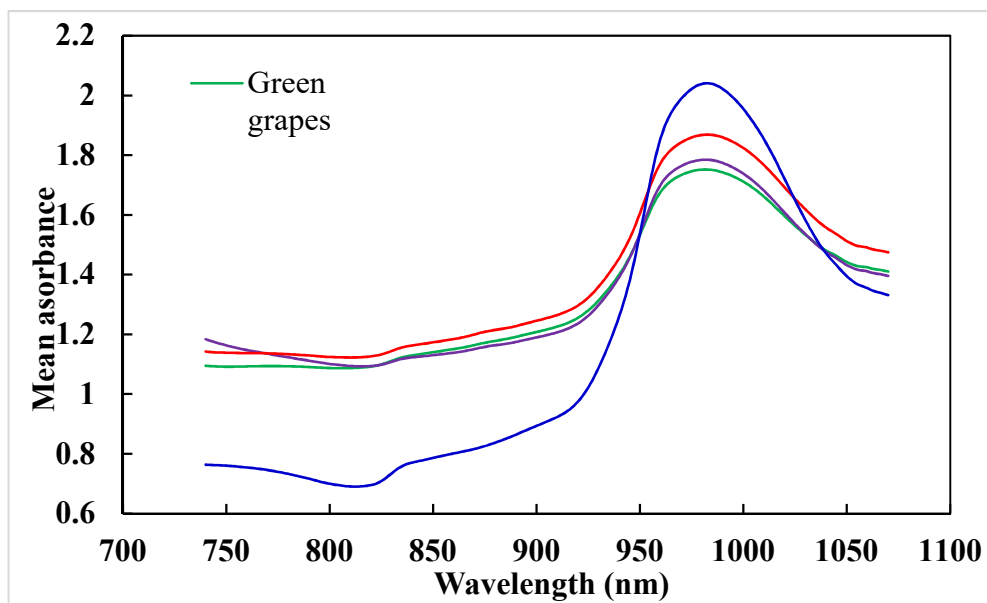


Figure 1. Absorbance spectra averaged per cultivar for 150 green grapes, 150 purple grapes, 150 red grapes and 150 peaches, acquired with the SCiO spectrometer.

Figure 2 shows the mean of absorbance spectra of 450 table grapes and 150 peach fruits acquired by the F-750 and SCiO spectrometers at NIR region 740–1070 nm, respectively. Although the absorbance intensity varied, all the spectra had similarities in their overall pattern and shape. It is seen that the spectra showed one broad absorbance peak around 975 nm, which can be associated with water and sugar absorption [37,38]. The raw spectral data also contain undesirable interferences such as overlapped bands, scattering and random noises, and therefore these spectra were subjected to pre-processing methods. The spectra that generated the combination of the minimum RMSE, higher R^2 and RPD, bias near zero, and optimized numbers of LV were considered for the PLSR modelling. As mentioned, for model development and performance evaluation for predicting DM and TSS for table grapes and peach, only the NIR range from 740 to 1070 nm was considered for both spectrometers, discarding the VIS wavelengths of F-750.

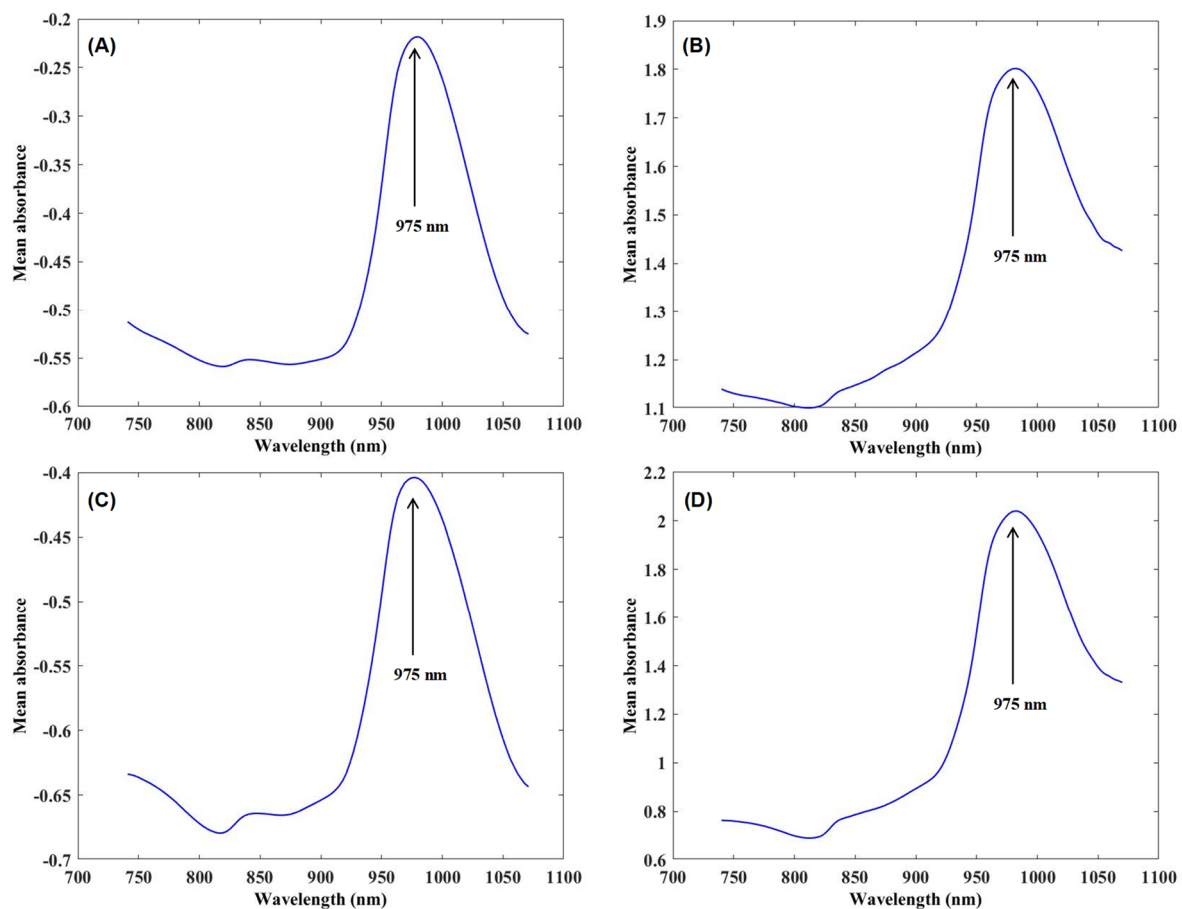


Figure 2. Mean original absorbance spectra for 450 table grapes acquired by (A) the F-750, (B) the SCiO spectrometers; and for 150 peaches acquired by (C) the F-750, and (D) the SCiO spectrometers.

3.1. PLSR Models for Predicting the DM and TSS of Table Grape and Peach Fruits

Calibration and prediction models based on PLSR to infer the DM and TSS of table grapes and peach fruits were developed in the range of 740–1070 nm region using the F-750 and SCiO spectrometers. The results obtained for the original and pre-treatment spectral data of both spectrometers in calibration and prediction models are shown in Table 3 for table grapes and peach. Regarding the different pre-processing techniques applied, the PLSR calibration model using OSC performed better for predicting table grape DM using the F-750 and SCiO spectrometers, which had the highest R^2 (0.79 and 0.75), lowest RMSEC (1.55 and 1.66), and highest RPD (2.17 and 2.02), and contained optimal number of LV (nine and 11). Similarly, the best PLSR calibration models were obtained for SNV spectra for predicting TSS in table grapes using both spectrometers, showing a very high value of R^2 (0.99 with F-750, and 0.97 with SCiO), RPD (8.96 and 5.87) and a fairly low value of RMSEC (0.36 and 0.55) with a larger number of LV (19 and 14) than for DM. The overall calibration results obtained in the original and pre-processing spectra were not noticeable predictors for DM and TSS in peach, but slightly better results were obtained in prediction (e.g., larger value of R^2 and RPD, and smaller value of RMSEP) using pre-processing techniques as shown in Table 4. The obtained results using SD pre-processing with eight LV and FD pre-processing with six LVs performed better for the F-750 spectrometer, and SG with nine LV and SNV with eight LV performed better for the SCiO spectrometer for the prediction of peach DM and TSS, respectively.

Table 3. Partial least-square regression calibration and prediction model results for table grape and peach quality attributes.

| Quality Attribute | Spectra | No. of LV | | Calibration | | | | | | Prediction | | | | | | | |
|------------------------------|------------|-----------|-----------|-------------|-------------|-------------|-------------|-------------|-------------|-------------|-------------|-------------|-------------|-------------|-------------|--------------|--------------|
| | | | | R^2 | | RMSEC | | RPD | | R^2 | | RMSEP | | RPD | | Bias | |
| | | | | F-750 | SCiO | F-750 | SCiO |
| DM (%) for Table Grapes | Original | 9 | 12 | 0.77 | 0.75 | 1.60 | 1.69 | 2.10 | 1.98 | 0.82 | 0.78 | 1.41 | 1.56 | 2.34 | 2.12 | -0.18 | -0.07 |
| | SNV | 9 | 11 | 0.79 | 0.77 | 1.54 | 1.62 | 2.17 | 2.07 | 0.80 | 0.78 | 1.52 | 1.55 | 2.17 | 2.13 | -0.31 | -0.17 |
| | OSC | 9 | 11 | 0.79 | 0.75 | 1.55 | 1.66 | 2.17 | 2.02 | 0.83 | 0.81 | 1.40 | 1.44 | 2.35 | 2.29 | -0.27 | -0.09 |
| | FD | 9 | 11 | 0.47 | 0.41 | 2.45 | 2.58 | 1.37 | 1.30 | 0.52 | 0.58 | 4.11 | 2.26 | 0.80 | 1.46 | 0.88 | 0.23 |
| | SD | 9 | 11 | 0.77 | 0.76 | 1.61 | 1.64 | 2.09 | 2.05 | 0.82 | 0.80 | 1.43 | 1.47 | 2.32 | 2.25 | -0.21 | -0.13 |
| | SG | 9 | 11 | 0.76 | 0.74 | 1.63 | 1.70 | 2.06 | 1.98 | 0.82 | 0.81 | 1.40 | 1.45 | 2.35 | 2.27 | -0.16 | -0.16 |
| DM (%) for Peach | Original | 8 | 12 | 0.60 | 0.61 | 2.02 | 1.99 | 1.58 | 1.60 | 0.72 | 0.58 | 2.32 | 1.89 | 1.24 | 1.53 | -0.30 | 0.23 |
| | SNV | 8 | 9 | 0.64 | 0.58 | 1.90 | 2.05 | 1.68 | 1.56 | 0.15 | 0.63 | 3.59 | 1.78 | 0.80 | 1.61 | 0.50 | 0.33 |
| | OSC | 8 | 9 | 0.64 | 0.58 | 1.91 | 2.05 | 1.67 | 1.55 | 0.30 | 0.65 | 2.85 | 1.71 | 1.00 | 1.68 | 0.47 | 0.29 |
| | FD | 8 | 9 | 0.61 | 0.57 | 1.99 | 2.09 | 1.60 | 1.53 | 0.64 | 0.45 | 33.6 | 2.44 | 0.09 | 1.18 | 13.1 | 1.00 |
| | SD | 8 | 9 | 0.60 | 0.63 | 2.00 | 1.93 | 1.59 | 1.65 | 0.81 | 0.61 | 1.28 | 1.80 | 2.24 | 1.60 | 0.01 | 0.28 |
| | SG | 8 | 9 | 0.59 | 0.56 | 2.04 | 2.11 | 1.56 | 1.51 | 0.17 | 0.67 | 3.32 | 1.66 | 0.86 | 1.74 | 0.48 | 0.24 |
| TSS (°Brix) for Table Grapes | Original | 20 | 15 | 0.98 | 0.95 | 0.50 | 0.71 | 6.41 | 4.54 | 0.97 | 0.96 | 0.53 | 0.72 | 5.99 | 4.41 | 0.02 | -0.04 |
| | SNV | 19 | 14 | 0.99 | 0.97 | 0.36 | 0.55 | 8.96 | 5.87 | 0.98 | 0.97 | 0.39 | 0.58 | 8.03 | 5.43 | 0.00 | -0.01 |
| | OSC | 19 | 14 | 0.99 | 0.95 | 0.39 | 0.70 | 8.36 | 4.58 | 0.98 | 0.96 | 0.43 | 0.71 | 7.33 | 4.45 | -0.02 | -0.05 |
| | FD | 19 | 14 | 0.67 | 0.54 | 1.86 | 2.16 | 1.73 | 1.45 | 0.48 | 0.21 | 4.41 | 3.13 | 0.72 | 1.00 | 0.33 | 0.72 |
| | SD | 19 | 14 | 0.98 | 0.95 | 0.42 | 0.70 | 7.74 | 4.61 | 0.98 | 0.96 | 0.42 | 0.72 | 7.48 | 4.39 | 0.00 | -0.07 |
| | SG | 19 | 14 | 0.98 | 0.94 | 0.40 | 0.77 | 7.98 | 4.20 | 0.98 | 0.95 | 0.41 | 0.77 | 7.74 | 4.09 | -0.02 | -0.00 |
| TSS (°Brix) for Peach | Original | 13 | 7 | 0.72 | 0.40 | 1.04 | 1.53 | 1.89 | 1.28 | 0.51 | 0.46 | 1.32 | 1.40 | 1.40 | 1.32 | 0.22 | 0.38 |
| | SNV | 6 | 8 | 0.52 | 0.52 | 1.35 | 1.35 | 1.45 | 1.45 | 0.48 | 0.55 | 1.32 | 1.25 | 1.40 | 1.48 | 0.18 | 0.15 |
| | OSC | 6 | 8 | 0.53 | 0.53 | 1.35 | 1.35 | 1.46 | 1.46 | 0.52 | 0.49 | 1.29 | 1.30 | 1.43 | 1.42 | 0.24 | 0.02 |
| | FD | 6 | 8 | 0.44 | 0.51 | 1.47 | 1.38 | 1.34 | 1.43 | 0.62 | 0.74 | 1.19 | 5.22 | 1.55 | 0.35 | 0.31 | 0.05 |
| | SD | 6 | 8 | 0.53 | 0.55 | 1.33 | 1.31 | 1.47 | 1.50 | 0.49 | 0.52 | 1.32 | 1.28 | 1.40 | 1.45 | 0.22 | -0.04 |
| | SG | 6 | 8 | 0.19 | 0.50 | 1.36 | 1.38 | 1.11 | 1.42 | 0.07 | 0.51 | 1.45 | 1.29 | 1.02 | 1.43 | -0.32 | 0.08 |

SNV = Standard Normal Variate, OSC = Orthogonal Signal Correction, FD = First Derivative, SD = Second Derivative, and SG = Smoothing using the Savitzky–Golay algorithm. Bolded figures indicate best performance models, depending on spectra preprocessing, and trait.

The calculated RMSECV values for PLSR is plotted as a function of the number of LVs in Figure 3. Overall, the number of LVs considered for model development were in the acceptable range for all of the models, because the number of samples within the calibration data set were ten times larger than the LVs [39]. However, the minimum RMSECV was observed in the 19th and 14th LVs for the prediction of TSS in table grapes using the F-750 and SCiO spectrometers, respectively. The latter indicates that a large number of factors were interpreted to construct the models. From Figure 3, it is seen that the first minimum RMSECV value was observed in the 7th LV (marked by blue dotted circle) to predict the TSS using the F-750, capturing 100% of the variance by the regressor and explaining 97.16% of its variance (Table 3). The difference of the RMSECV between the 7th and 8th LVs and thereafter were relatively low and insignificant, indicating that LVs above seven might contain irrelevant information and will cause an over fitted model. Hence, 7 were the optimal number of LVs chosen to predict table grape TSS using the F-750 spectrometer. Similarly, to avoid irrelevant information and model over fitting, the optimal number of LVs (marked by blue dot circle) to predict the TSS in table grapes using the SCiO spectrometer was equal to 9.

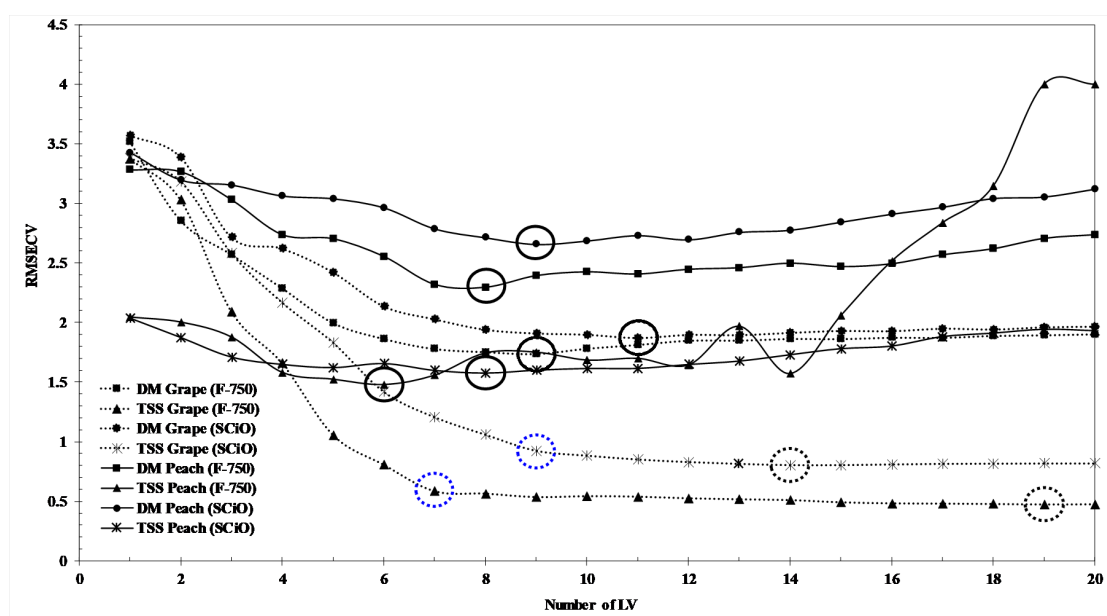


Figure 3. Number of latent variables (LV) versus root-mean square error of cross-validation (RMSECV) values in the partial least-squares regression (PLSR) calibration model to predict dry matter (DM) and total soluble solids (TSS) in table grapes and peach fruits using the F-750 and SCiO spectrometers. Circles indicate optimized number of LV for each model; when two circled points are present in a calibration model, blue dot circle indicates further adjustment to avoid over fitting.

Table 4. Total percent variance of X and Y explained by the optimum number of latent variables (LV) captured by the regression model using PLSR.

| Fruit | Meter | Constituents Preprocessing | | LV | RMSECV | X-Block | Y-Block |
|--------------|-------|----------------------------|-----|----|--------|---------|---------|
| Table grapes | F-750 | DM | OSC | 9 | 1.736 | 99.99 | 78.66 |
| | | TSS | SNV | 7 | 0.584 | 100.00 | 97.16 |
| | SCiO | DM | OSC | 11 | 1.871 | 100.00 | 75.46 |
| | | TSS | SNV | 9 | 0.924 | 100.00 | 95.35 |
| Peach | F-750 | DM | SD | 8 | 2.294 | 100.00 | 60.10 |
| | | TSS | FD | 6 | 1.478 | 99.99 | 43.48 |
| | SCiO | DM | SG | 9 | 2.656 | 100.00 | 55.71 |
| | | TSS | SNV | 8 | 1.576 | 100.00 | 52.09 |

3.2. Model Prediction Performance to Infer DM Content in Table Grapes and Peach

Figure 4A–D show the results for the prediction of table grape DM in PLSR regression using the best calibration model developed by OSC spectra using the F-750 and SCiO spectrometers, respectively. These figures demonstrated that good results were obtained for table grape DM prediction using both produce quality spectrometers. These results are aligned with the ones obtained by [24] using also the F-750 and SCiO spectrometers for DM assessment on apples and kiwis, with R^2 values between 0.8 and 0.95. In the case of the F-750 spectrometer, the coefficient of determination, RMSEP, and RPD for the DM prediction set varied from 0.52 to 0.83, 1.40 to 4.11, and 0.80 to 2.35, respectively (Table 3). As seen in Table 4 the application of pre-processing techniques on the PLSR model had less effect on prediction performance but the calibration model using OSC was slightly improved the model's predictive power with $R^2 = 0.83$, RMSEP = 1.40, RPD = 2.35, and bias = -0.27 (Figure 4B). On the other-hand, R^2 , RMSEP, and RPD for the DM prediction set using the SCiO spectrometer varied between 0.58–0.81, 1.45–2.66, and 1.46–2.29, respectively (Table 3). The PLSR model with OSC and smoothing spectra showed the same coefficient of determination ($R^2 = 0.81$) but considering other statistical parameters, the PLSR model with OSC (Figure 4D) was chosen as the best model for the prediction of DA in table grapes using the SCiO spectrometer. There is no previous study that addressed the direct measurement of DM in fresh table grapes using NIR spectroscopy. However, ref. [40] have reported the measurement of DM in homogenized table grape samples using the NIR region from 1100 to 2500 nm. They found better prediction results ($R^2 = 0.90$, SEP = 1.34, RPD = 2.2, and bias = 0.48) in their NIR-based PLSR model. Figure 4E–H show the results of PLSR models developed for the prediction of peach DM using the F-750 and SCiO spectrometers, respectively. These figures and Table 4 revealed that for both spectrometers, improved results were obtained in the prediction set than in calibration after applying pre-processing. The R^2 and RPD were achieved at 0.81 and 2.24 for the F-750 spectrometer using the best PLSR model in SD spectra and eight LVs (Figure 4F) and 0.67 and 1.74 for the SCiO spectrometer using the best PLSR model in SG spectra and nine LV (Figure 4H). One study was found that measured the DM content in peach using NIR technique but obtained unsatisfactory results [19]. Considering the model chemometric indicators, overall, the F-750 spectrometer performed comparatively better than the SCiO spectrometer for measuring the DM in peach fruits; this can be associated with a lower variability of measurements, as explained later in Section 3.4.

3.3. Model Prediction Performance to Infer TSS Content in Table Grapes and Peach

The models developed with SNV spectra to predict the TSS in table grapes using the F-750 and SCiO spectrometers achieved an excellent value for the coefficient of determination for both spectrometers across the range of 4.35–21.1 °Brix. Figure 5A–D shows the results of correlation between the measured and predicted values of table grape TSS in calibration and prediction using the PLSR model and SNV pre-processing. The application of SNV pre-processing technique on the PLSR model significantly improved the results of both calibration and prediction. In particular, the value of RPD increased solidly in comparison with original spectra. In prediction, the R^2 , RMSEP, RPD, and bias was obtained at 0.97, 0.53, 5.95, and 0.01, respectively, using seven LV for the F-750 spectrometer, and was obtained at 0.95, 0.70, 4.48, and 0.08, respectively, using nine LV for the SCiO spectrometer, evidently showing excellent model performance [41]. These results also demonstrated that the developed model for direct measurement of TSS in fresh grapes produced better prediction results when compared with the results obtained by [42] ($R^2 = 0.95$, RMSEP = 1.011), [15] ($R^2 = 0.91$, RMSEP = 1.42, RPD = 3.36), [43] ($R^2 = 0.94$, SECV = 1.0, RPD = 4.12), and [18] ($R^2 = 0.82$, RMSEP = 1.48). RPD is one of the important model performance evaluation chemometric indexes and the higher RPD confirmed the model prediction accuracy and robustness [9]. Considering the value of RPD, it is also seen that the F-750 spectrometer performed best for measuring TSS in table grape fruits than the SCiO spectrometer. Figure 5E–H shows the results of the PLSR models of TSS prediction in peach using the F-750 and SCiO spectrometers, respectively. The R^2 , RMSEP, RPD, and bias of the external validation set were 0.62, 1.19, 1.55, and 0.31, respectively, for F-750 and 0.55, 1.25, 1.48, and

0.15, respectively, for the SCiO spectrometer (Table 4). These model evaluation indexes indicated that the PLSR prediction model for TSS in fresh peach were not satisfactory for either of the spectrometers and had poor predictive performance in comparison to table grapes. Two reasons may explain this result: First, the number of samples (berries) in the grape models was three times higher than in the case of peaches; second, the maturity state of some of the peaches was quite high (too ripe), resulting in a narrower range of TSS (4.35–21.1 Brix for grapes, and 21.1–17.85 Brix for peaches, Table 1).

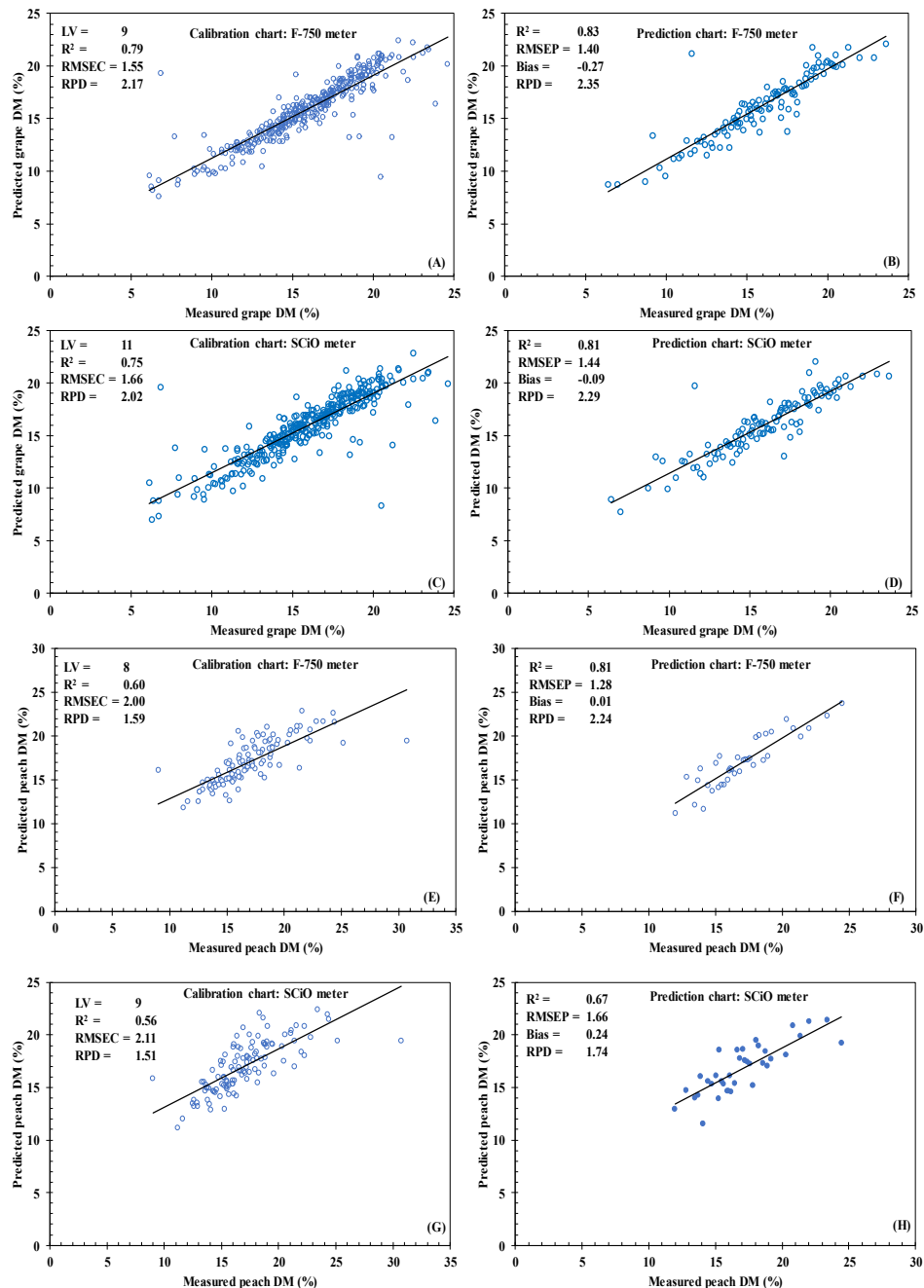


Figure 4. Scatter plot of measured versus predicted dry matter (DM) values of table grapes (A–D) and peach (E–H) calculated using the best PLSR calibration model for the F-750 and SCiO spectrometers. The black line represents the linear correlation between the measured values obtained from the reference quality attribute and their prediction by the model. LV = latent variables, R^2 = coefficient of determination, RMSEC = root mean squared error of calibration, RMSEP = root mean squared error of prediction, RPD = performance to deviation ratio.

With the aim of summarizing these results, it can be stated that the chemometric indexes for DM and TSS models showed acceptable results and demonstrated that the NIR spectra region (740–1100 nm) coupled with PLSR regression could effectively predict the DM and TSS across the range of 6.12–24.61% and 4.35–21.1 °Brix, respectively, in table grapes using the F-750 and SCiO spectrometers. Both quality spectrometers therefore could be used to non-destructively determine DM and TSS quality attributes in fresh table grapes. The PLSR results of fresh peach DM and TSS were poorly predicted by both spectrometers. Based on the chemometric indicators of the DM prediction set, the F-750 spectrometer produced relatively better results than SCiO with $R^2 = 0.81$, RMSEP = 1.28, and RPD = 2.24 and could potentially be used for determination of DM in peach using PLSR regression. Overall, it can be inferred that the F-750 had a higher performance in comparison to the SCiO for the prediction of DM and TSS; again, this can be due to more stable spectral readings, according to results of Section 3.4.

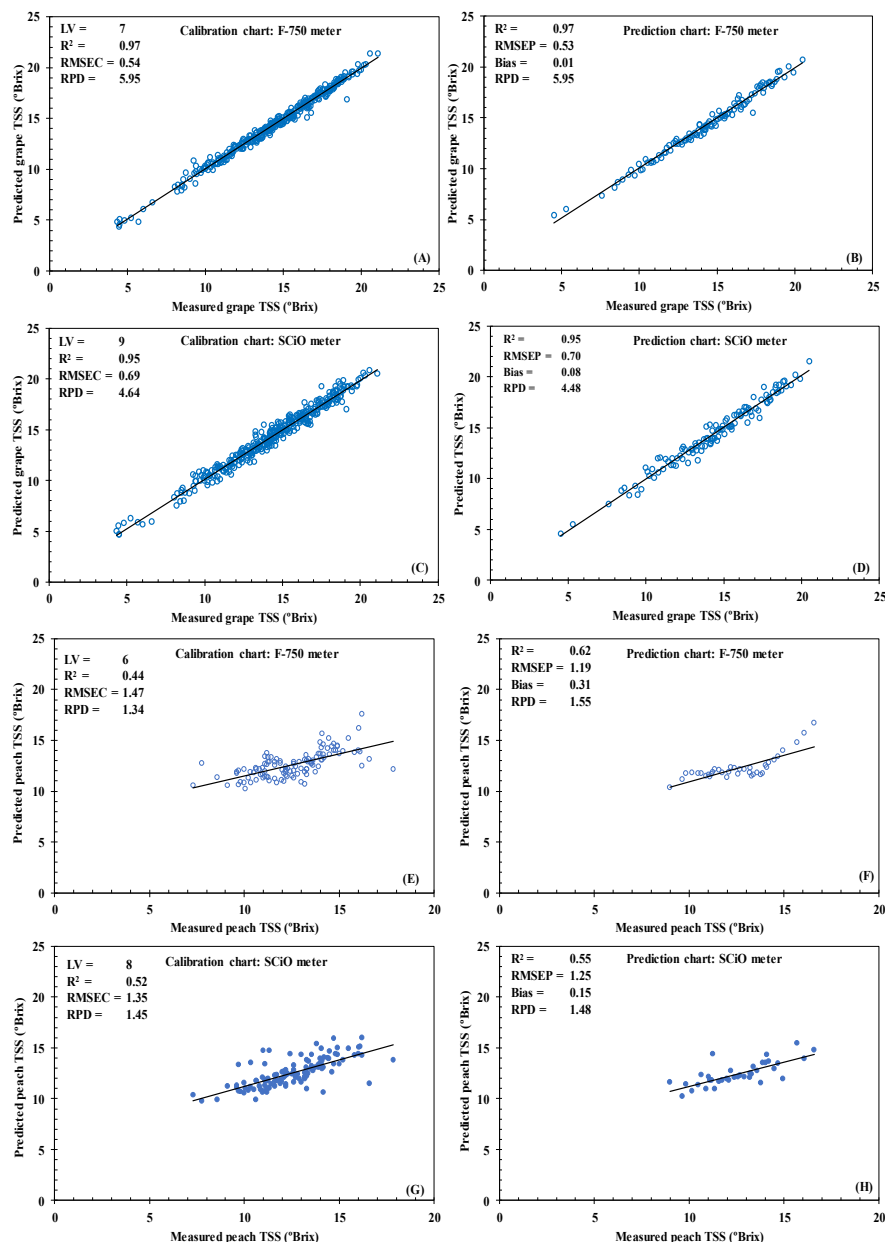


Figure 5. Scatter plot of measured versus predicted total soluble solids (TSS) values of table grapes (A–D) and peach (E–H) calculated using the best PLSR calibration model for the F-750 and SCiO spectrometers. The black line represents the linear correlation between the measured values obtained from the reference quality attribute and their prediction by the model.

3.4. Performance Evaluation Using Reference Spheres

From the overall comparison of the models obtained using the two produce quality meters, it is suggested that the F-750 DM and TSS prediction performance is higher in comparison to the SCiO and can be suitable to non-destructively measure fruit quality attributes. However, the performance of both meters was further investigated using a solid object (inert reference) to confirm the PLS results.

The spectra acquisition with biological samples is often complicated and contains high- and/or low-frequency interferences and irrelevant information due to non-uniform distribution of light over the surface [29]. Hence, a wavelength by wavelength comparison was made between the spectrum of F-750 and SCiO meters obtained using a standard solid object (white Teflon sphere). The average coefficient of variation (CV) of the measured spectrums for each temperature is shown in Table 5. It is seen that the SCiO spectrometer yielded a higher variation per wavelength within the spectrum range acquired at each temperature, and as well as between the spectrum acquired at different room temperatures with an overall mean variation equal to 18.39%. The percent of variation per wavelength within and between the spectrums observed was almost zero for F-750, indicating that the acquired spectra using this meter apparently showed a similar pattern for all three different room conditions, and the lowest variability between the spectrometers.

Table 5. Summary of the average coefficient of variation of measured Teflon spectra in absorbance values.

| Meter | Coefficient of Variation (%) | | | Overall Average |
|-------|------------------------------|-------|-------|-----------------|
| | 0 °C | 10 °C | 20 °C | |
| SCiO | 13.91 | 24.99 | 16.26 | 18.39 |
| F-750 | 0.41 | 0.13 | 0.15 | 0.23 |

When inferring the SNR of the acquired absorbance Teflon spectra with both spectrometers (Figure 6), strong differences between the devices can be observed. Highly noisy signals can be observed near the limits of their wavelength ranges, and even though both meters react to sample temperature variations at different levels, both show stable signals in the NIR region used to build prediction PLSR models in this study (740 to 1070 nm). However, the SNR in the case of the F-750 is one hundred times higher than for the SCiO, potentially affecting the performance of the PLSR prediction models. The higher noise in the F-750 spectrometer did not seem to affect its overall prediction performance as it is still better than the SCiO performance. This variation can be potentially due to the intrinsic design of each of the spectrometers, including the incident light intensity and type, and additional electrical components.

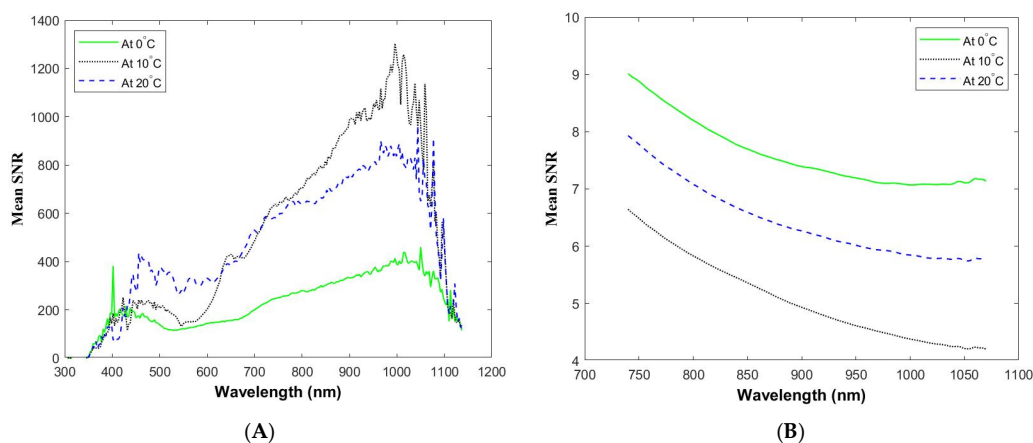


Figure 6. Mean signal-to-noise ratio (SNR) of Teflon absorbance spectra measured at different room temperatures with the F-750 meter (A) and with the SCiO meter (B), across their respective full wavelength range.

4. Conclusions

Two NIR produce quality spectrometers were investigated in this study to evaluate their performance to non-invasively determine quality attributes for three table grape cultivars ('Autumn Royal', 'Timpson', and 'Sweet Scarlet') and one peach cultivar ('Cassie') using PLSR models in the 740–1070 nm wavelength range and various pre-processing techniques. Results indicated that both spectrometers performed well in predicting DM ($R^2 > 80\%$) and TSS ($R^2 > 90\%$) contents in fresh table grapes. Regarding peach, the F-750 spectrometer performed comparatively better than the SCiO spectrometer and yielded high prediction accuracy DM ($R^2 = 0.81$ and RPD = 2.24). Overall, both spectrometers were not effective in predicting the TSS of fresh peach. Among the two spectrometers, the F-750 spectrometer seems suitable for practical use and could readily be used for field applications for predicting the quality attributes in fresh table grapes and peach fruits. To improve the modeling performance and to confirm the reliability of both spectrometers to predict quality attributes of fresh peaches, especially the content of TSS, further studies are recommended.

Author Contributions: Conceptualization, D.C.S., I.R.D.-G. and C.V.; methodology, C.V., M.A.M. and I.R.D.-G.; software, M.A.M., C.V. and I.R.D.-G.; validation, M.A.M., C.V., A.K. and I.R.D.-G.; formal analysis and research, M.A.M. and C.V.; data curation, M.A.M. and C.V.; writing—original draft preparation, M.A.M.; writing—review and editing, M.A.M., C.V. and I.R.D.-G.; visualization, M.A.M.; supervision, and project administration, I.R.D.-G. and D.C.S.; funding acquisition, C.V. and I.R.D.-G. All authors have read and agreed to the published version of the manuscript.

Funding: This research received no external funding, except for the mobility grant mentioned in acknowledgements.

Acknowledgments: The research stay of Valero at UC Davis was possible due to a Mobility Grant for senior academics funded in 2017 by the Spanish Ministry of Education, Culture and Sport, Gobierno de España (SIA code: IUE—Salvador de Madariaga, number 998759). Valero also wants to acknowledge the support and invaluable help received from the University of California-Davis, especially from the staff at the BAE department.

Conflicts of Interest: The authors declare no conflict of interest.

References

1. California Department of Food and Agriculture. *California Agricultural Statistics Review, 2017–2018*; California Department of Food and Agriculture: Sacramento, CA, USA, 2018; p. 118.
2. El-Mesery, H.S.; Mao, H.; Abomohra, A.E.F. Applications of non-destructive technologies for agricultural and food products quality inspection. *Sensors* **2019**, *19*, 846. [[CrossRef](#)]
3. Khodabakhshian, R.; Emadi, B.; Khojastehpour, M.; Golzarian, R.; Sazgarnia, A. Non-destructive evaluation of maturity and quality parameters of pomegranate fruit by visible/near infrared spectroscopy. *Int. J. Food Prop.* **2017**, *20*, 41–52. [[CrossRef](#)]
4. Santos, L.R.D.; Zangirolami, M.D.S.; Silva, N.O.; Valderrama, P.; Março, P.H. Rapid non-invasive assessment of quality parameters in ground soybean using near-infrared spectroscopy. *Pesqui. Agropecuária Bras.* **2018**, *53*, 97–104. [[CrossRef](#)]
5. Wang, H.; Peng, J.; Xie, C.; Bao, Y.; He, Y. Fruit quality evaluation using spectroscopy technology: A review. *Sensors* **2015**, *15*, 11889–11927. [[CrossRef](#)]
6. Pasquini, C. Near infrared spectroscopy: Fundamentals, practical aspects and analytical applications. *J. Braz. Chem. Soc.* **2003**, *14*, 198–219. [[CrossRef](#)]
7. Nicolai, B.M.; Beullens, K.; Bobelyn, E.; Peirs, A.; Saeys, W.; Theron, K.I.; Lammertyn, J. Nondestructive measurement of fruit and vegetable quality by means of NIR spectroscopy: A review. *Postharvest Biol. Technol.* **2007**, *46*, 99–118. [[CrossRef](#)]
8. Rinnan, Å.; Berg, F.V.D.; Engelsen, S.B. Review of the most common pre-processing techniques for near-infrared spectra. *Trends Anal. Chem.* **2009**, *28*, 1201–1222. [[CrossRef](#)]
9. Viegas, T.R.; Mata, A.L.M.L.; Duarte, M.A.M.L.; Lima, K.A.M.G. Determination of quality attributes in wax jambu fruit using NIRS and PLS. *Food Chem.* **2016**, *190*, 1–4. [[CrossRef](#)]
10. Jaleh, B.; Fakhri, P. *Infrared and Fourier Transform Infrared Spectroscopy for Nanofillers and Their Nanocomposites*; Elsevier Inc.: Amsterdam, The Netherlands, 2016; pp. 112–129.

11. Abdi, H. Partial least squares regression and projection on latent structure regression (PLS Regression). *Wiley Interdiscip. Rev. Comput. Stat.* **2010**, *2*, 97–106. [[CrossRef](#)]
12. Rinnan, Å. Pre-processing in vibrational spectroscopy—when, why and how. *Anal. Methods* **2014**, *6*, 7124–7129. [[CrossRef](#)]
13. Dale, L.M.; Thewis, A.; Rotar, I.; Pierna, J.A.F.; Boudry, C.; Vidican, R.M.; Baeten, V. Chemometric Tools for NIRS and NIR Hyperspectral Imaging. *Bull. Uasvm Agric.* **2012**, *69*, 70–76.
14. Caramês, E.T.S.; Alamar, P.D.; Poppi, R.J.; Pallone, J.A.L. Quality control of cashew apple and guava nectar by near infrared spectroscopy. *J. Food Compos. Anal.* **2017**, *56*, 41–46. [[CrossRef](#)]
15. Urraca, R.; Sanz-Garcia, A.; Tardaguila, J.; Diago, M.P. Estimation of total soluble solids in grape berries using a hand-held NIR spectrometer under field conditions. *J. Sci. Food Agric.* **2016**, *96*, 3007–3016. [[CrossRef](#)]
16. Barnaba, F.E.; Bellincontro, A.; Mencarelli, F. Portable NIR-AOTF spectroscopy combined with winery FTIR spectroscopy for an easy, rapid, in-field monitoring of Sangiovese grape quality. *J. Sci. Food Agric.* **2014**, *94*, 1071–1077. [[CrossRef](#)]
17. Fernández-Navales, J.; López, M.I.; Sánchez, M.T.; García-Mesa, J.A.; González-Caballero, V. Assessment of quality parameters in grapes during ripening using a miniature fiber-optic near-infrared spectrometer. *Int. J. Food Sci. Nutr.* **2009**, *60*, 265–277. [[CrossRef](#)]
18. Guidetti, R.; Beghi, R.; Bodria, L. Evaluation of grape quality parameters by a simple VIS/NIR system. *Trans. ASABE* **2010**, *53*, 477–484. [[CrossRef](#)]
19. Costa, G.; Noferini, M.; Fiori, G.; Miserochi, O.; Bregoli, A.M. NIRS evaluation of peach and nectarine fruit quality in pre-and post-harvest conditions. *Acta Hortic.* **2002**, *592*, 593–599. [[CrossRef](#)]
20. Fu, X.P.; Ying, Y.B.; Zhou, Y.; Xie, L.J.; Xu, H.R. Application of NIR spectroscopy for firmness evaluation of peaches. *J. Zhejiang Univ. Sci. B* **2008**, *9*, 552–557. [[CrossRef](#)]
21. Kawano, S.; Watanabe, H.; Iwamoto, M. Determination of Sugar Content in Intact Peaches by Near Infrared Spectroscopy with Fiber Optics in Interactance Mode. *Engei Gakkai Zasshi* **1992**, *61*, 445–451. [[CrossRef](#)]
22. Uwadaira, Y.; Sekiyama, Y.; Ikehata, A. An examination of the principle of non-destructive flesh firmness measurement of peach fruit by using VIS-NIR spectroscopy. *Heliyon* **2018**, *4*, e00531. [[CrossRef](#)]
23. Guillemain, A.; Dégardin, K.; Roggo, Y. Performance of NIR handheld spectrometers for the detection of counterfeit tablets. *Talanta* **2017**, *165*, 632–640. [[CrossRef](#)]
24. Kaur, H.; Künnemeyer, R.; McGlone, A. Comparison of hand-held near infrared spectrophotometers for fruit dry matter assessment. *J. Near Infrared Spectrosc.* **2017**, *25*, 267–277. [[CrossRef](#)]
25. McGonigle, A.J.S.; Wilkes, T.C.; Pering, T.D.; Willmott, J.R.; Cook, J.M.; Mims, F.M.; Parisi, A.V. Smartphone Spectrometers. *Sensors* **2018**, *18*, 223. [[CrossRef](#)]
26. Rateni, G.; Dario, P.; Cavallo, F. Smartphone-Based Food Diagnostic Technologies: A Review. *Sensors* **2017**, *17*, 1453. [[CrossRef](#)]
27. Kosmowski, F.; Worku, T. Evaluation of a miniaturized NIR spectrometer for cultivar identification: The case of barley, chickpea and sorghum in Ethiopia. *PLoS ONE* **2018**, *13*, e0193620. [[CrossRef](#)]
28. Gupta, S.D.; Ibaraki, Y. *Plant Image Analysis*; Taylor & Francis Group: Boca Raton, FL, USA, 2015; pp. 83–93.
29. Johnsen, S. How to measure color using spectrometers and calibrated photographs. *J. Exp. Biol.* **2016**, *219*, 772–778. [[CrossRef](#)]
30. Bona, E.; Março, P.H.; Valderrama, P. Chapter 4—Chemometrics Applied to Food Control. In *Food Control and Biosecurity*; Elsevier Inc.: Amsterdam, The Netherlands, 2018; pp. 105–133.
31. Fluvia Sabio, S. NIR Techniques and Chemometric Data Analysis Applied to Food Adulteration Detection. Master’s Thesis, Universitat Politècnica de Catalunya, Barcelona, Spain, 2015.
32. Zhao, N.; Wu, Z.-S.; Zhang, Q.; Shi, X.-Y.; Ma, Q. Optimization of Parameter Selection for Partial Least Squares Model Development. *Nat. Publ. Group* **2015**, *5*, 1–10. [[CrossRef](#)]
33. Gutierrez, D. Ask a Data Scientist: The Bias vs. Variance Tradeoff. Available online: <https://insidebigdata.com/2014/10/22/ask-data-scientist-bias-vs-variance-tradeoff/> (accessed on 25 March 2019).
34. Santos, P.M.; Colnago, L.A. Comparison Among MIR, NIR, and LF-NMR Techniques for Quality Control of Jam Using Chemometrics. *Food Anal. Methods* **2018**, *11*, 2029–2034. [[CrossRef](#)]
35. Souza, D.; Azevedo, J.; Pallone, L.; Jesus, R. Fourier transform near-infrared spectroscopy (FT-NIRS) application to estimate Brazilian soybean [*Glycine max* (L.) Merrill] composition. *FRIN* **2013**, *51*, 53–58.

36. Walther, B.A.; Moore, J.L. The concepts of bias, precision and accuracy, and their use in testing the performance of species richness estimators, with a literature review of estimator performance. *Ecography* **2005**, *28*, 815–829. [[CrossRef](#)]
37. Clark, C.J.; McGlone, V.A.; Requejo, C.; White, A.; Woolf, A.B. Dry matter determination in ‘Hass’ avocado by NIR spectroscopy. *Postharvest Biol. Technol.* **2003**, *29*, 301–308. [[CrossRef](#)]
38. Omar, A.F.; Atan, H.; Matjafri, M.Z. Peak response identification through near-infrared spectroscopy analysis on aqueous sucrose, glucose, and fructose solution. *Spectrosc. Lett.* **2012**, *45*, 190–201. [[CrossRef](#)]
39. Lammertyn, J.; Peirs, A.; Baerdemaeker, J.D.; Nicolai, B. Light penetration properties of NIR radiation in fruit with respect to non-destructive quality assessment. *Postharvest Biol. Technol.* **2000**, *18*, 121–132. [[CrossRef](#)]
40. Cozzolino, D.; Cynkar, W.U.; Damberg, R.G.; Mercurio, M.D.; Smith, P.A. Measurement of condensed tannins and dry matter in red grape homogenates using near infrared spectroscopy and partial least squares. *J. Agric. Food Chem.* **2008**, *56*, 7631–7636. [[CrossRef](#)]
41. Williams, P.C.; Norris, K.H. *Near-Infrared Technology: In the Agricultural and Food Industries*, 2nd ed.; American Association of Cereal Chemists: St. Paul, MN, USA, 2001; pp. 145–169.
42. Fernández-Navales, J.; Tardáguila, J.; Gutiérrez, S.; Diago, M.P. On-The-Go VIS SW– NIR spectroscopy as a reliable monitoring tool for grape composition within the vineyard. *Molecules* **2019**, *24*, 2795. [[CrossRef](#)]
43. González-Caballero, V.; Pérez-Marín, D.; López, M.I.; Sánchez, M.T. Optimization of NIR spectral data management for quality control of grape bunches during on-vine ripening. *Sensors* **2011**, *11*, 6109–6124. [[CrossRef](#)]



© 2020 by the authors. Licensee MDPI, Basel, Switzerland. This article is an open access article distributed under the terms and conditions of the Creative Commons Attribution (CC BY) license (<http://creativecommons.org/licenses/by/4.0/>).